

$\Sigma^\pm$  Lifetime and the Branching Ratio  $B_{\Sigma^+} \equiv (\Sigma^+ \rightarrow \pi^+ + n) / (\Sigma^+ \rightarrow \text{All})^*$

C. Y. CHANG†

Columbia University, New York, New York

(Received 23 February 1966)

Using 11 000 charged  $\Sigma$ 's produced from  $K^- + p \rightarrow \Sigma^\pm + \pi^\mp$  interactions taking place in the 30-in. Columbia-BNL hydrogen bubble chamber, we have determined the  $\Sigma^\pm$  lifetimes and the branching ratio  $B_{\Sigma^+} \equiv (\Sigma^+ \rightarrow \pi^+ + n) / (\Sigma^+ \rightarrow \text{all})$ . By means of a least-squares fit to the differential decay distributions for the in-flight sigma decays, the following values were obtained:  $\tau_{\Sigma^+} = (0.830 \pm 0.018) \times 10^{-10}$  sec,  $\tau_{\Sigma^-} = (1.666 \pm 0.026) \times 10^{-10}$  sec, and  $B_{\Sigma^+} = 0.46 \pm 0.02$ .

I. INTRODUCTION

PRECISE determination of the fundamental quantities, such as lifetimes, branching ratios, etc., associated with the nonleptonic decays of the strange particles is currently receiving considerable interest, basically because there exists no satisfactory theory for a complete description of such a decay mechanism. Nevertheless, quite a few features observed in this field can be successfully interpreted with certain phenomenological rules, among which the  $|\Delta I| = \frac{1}{2}$  rule is of substantial interest. The  $|\Delta I| = \frac{1}{2}$  rule allows only those decay transitions in which the change in the total isotopic spin of the strongly interacting particles is  $\frac{1}{2}$ .<sup>1</sup> With the  $|\Delta I| = \frac{1}{2}$  rule, and the fact that the  $\Sigma$  has isotopic spin 1, which permits its decay into a state of isotopic spin of  $\frac{1}{2}$  or  $\frac{3}{2}$ , it is then convenient, following Gell-Mann and Rosenfeld,<sup>2</sup> to represent each  $\Sigma \rightarrow \pi N$  amplitude by a vector  $\mathbf{M}$  in an  $(S, P)$  plane<sup>3</sup>; there is then a triangular relationship between these vectors, namely

$$\sqrt{2}\mathbf{M}_0 + \mathbf{M}_+ = \mathbf{M}_-, \tag{1}$$

for the three decays

$$\Sigma^+ \rightarrow \pi^+ + n \quad \mathbf{M}_+, \tag{2a}$$

$$\Sigma^- \rightarrow \pi^- + n \quad \mathbf{M}_-, \tag{2b}$$

$$\Sigma^+ \rightarrow \pi^0 + p \quad \mathbf{M}_0. \tag{2c}$$

Clearly, this relationship is much less definitive than the restrictions imposed by  $|\Delta I| = \frac{1}{2}$  on the branching ratios of  $\Lambda$  and  $\Xi$  nonleptonic decays.<sup>2</sup> However, there exists a great variety of experimental information for  $\Sigma^\pm$ ; it is quite relevant that by collecting these data one can investigate the validity of  $|\Delta I| = \frac{1}{2}$  for the nonleptonic decays of  $\Sigma^\pm$  in various ways. So far the

situation remains quite unclear; it seems that no definite conclusion has yet been drawn in the current reviews.<sup>4-6</sup> More precise measurements for these fundamental parameters associated with  $\Sigma^\pm \rightarrow \pi N$  decays therefore seem very desirable.

The  $\Sigma^\pm$  decay rates used in the most recent test<sup>7</sup> of the validity of  $|\Delta I| = \frac{1}{2}$  rule were calculated based on the latest published values of the  $\Sigma$  lifetimes and the branching ratio<sup>8</sup>

$$B_{\Sigma^+} \equiv \frac{(\Sigma^+ \rightarrow \pi^+ + n)}{(\Sigma^+ \rightarrow \text{all})}.$$

This determination was carried out with 1488  $\Sigma^-$ 's and 732  $\Sigma^+$ 's in a liquid-hydrogen bubble chamber where only  $\Sigma$  decays with a  $\Sigma$  length larger than 0.1 cm were used. The lifetimes found in that experiment were systematically lower than the earlier values obtained from nuclear emulsions.<sup>9</sup> Statistically, the 0.1-cm hyperon length cutoff could have rejected a substantial amount of the available information (for  $K^-$  capture at rest, the maximum length for  $\Sigma^+$  and  $\Sigma^-$  in liquid hydrogen are 1.2 and 0.9 cm, respectively; therefore the 0.1-cm length cutoff should reject  $\sim 24\%$   $\Sigma^+$  and  $\sim 13\%$   $\Sigma^-$  events). On the other hand, even with such a criterion, which is obviously not systematic in itself, the ambiguity between  $\Sigma^+$  and  $\Sigma^-$  still cannot be completely removed.<sup>8</sup> It was also noticed that (a) the effect of nuclear interactions of  $(\Sigma^- + p)$  on the determination of  $\Sigma^-$  lifetime was considerably large as compared with the statistical error for  $\tau_{\Sigma^-}$  quoted in Ref. 8. This effect must be properly treated. (b) The scanning bias for the  $\Sigma^+ \rightarrow p + \pi^0$  events due to short length protons was completely ignored by the previous experiments. Therefore the present experiment, with higher statistics (7820  $\Sigma^-$ 's and 3140  $\Sigma^+$ 's) and improved

\* Research supported in part by the U. S. Atomic Energy Commission.

† Present address: Department of Physics, Syracuse University, Syracuse, New York.

<sup>1</sup> M. Gell-Mann and A. Pais, in *Proceedings of the International Conference on High Energy Physics at Glasgow* (Pergamon Press, Inc., London, 1955). See also, *Proceedings of the Fifth Annual Conference on High Energy Physics* (Interscience Publishers, Inc., New York, 1955), p. 136.

<sup>2</sup> M. Gell-Mann and A. H. Rosenfeld, *Ann. Rev. Nucl. Sci.* **7**, 407 (1957).

<sup>3</sup>  $S$  and  $P$  are the phenomenological  $S$ - and  $P$ -wave amplitudes for the  $\Sigma \rightarrow \pi N$  decays.

<sup>4</sup> J. Steinberger, lectures given at the International School of Physics, "Enrico Fermi," Varenna, Italy, 1964 (unpublished). See also Nevis Report No. 125 (unpublished).

<sup>5</sup> R. H. Dalitz, The Brookhaven International Conference on Fundamental Aspects of Weak Interactions, September, 1963 (unpublished).

<sup>6</sup> F. S. Crawford, Jr., in *Proceedings of the International School of Physics, "Enrico Fermi," Fundamental Particles* (Academic Press Inc., New York, 1963).

<sup>7</sup> P. Franzini and D. Zanello, *Phys. Letters* **5**, 254 (1963).

<sup>8</sup> W. E. Humphrey and R. R. Ross, *Phys. Rev.* **127**, 1305 (1962).

<sup>9</sup> W. H. Barkas, J. N. Dyer, C. J. Mason, N. A. Nickols, and F. M. Smith, *Phys. Rev.* **124**, 1209 (1961).

technique, was devoted to a precise measurement of the  $\Sigma$  lifetime  $\tau_{\Sigma^*}$  and the branching ratio  $B_{\Sigma^*}$ . The results presented here are essentially free from the biases mentioned above.

The experimental technique employs the capture of  $K^-$  mesons at rest in a central region of the Columbia-BNL 30-in. hydrogen bubble chamber via the reaction  $K^- + p \rightarrow \Sigma^{\pm} + \pi^{\mp}$ . The analysis consists of an investigation of all the two-prong  $K^- + p$  interaction events taking place in the chamber. The main features of this experiment can be summarized below:

(i) For  $K^-$  capture at rest, the  $\Sigma$  hyperon produced in the two-body final state has a well-known initial momentum in the laboratory that permits an accurate determination of the  $\Sigma$  decay times.

(ii) The investigation of all two-prong  $K^- + p$  interaction events taking place in the chamber reduces the scanning biases introduced by short-length  $\Sigma$ 's to a minimum.

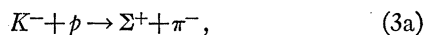
## II. EXPERIMENTAL PROCEDURES

### A. The Apparatus

This experiment was carried out by using part of the 400 000 pictures taken in 1963 at the BNL AGS with the 30-in. Columbia-BNL hydrogen bubble chamber exposed to a low-energy  $K^-$  beam.<sup>10</sup> Details of the beam features and the 30-in. chamber are described elsewhere.<sup>10,11</sup>

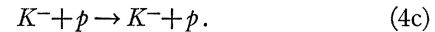
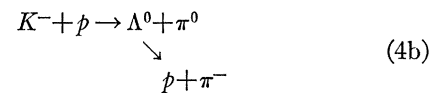
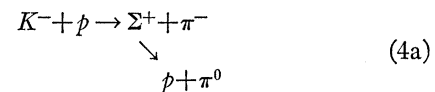
### B. Selection, Measurement, and Geometrical Reconstruction of the Events

A low-momentum separated  $K^-$  beam ( $P_{\text{lab}} \leq 250$  MeV/c) incident on a hydrogen bubble chamber can initiate the following reactions:



Reactions (3a) and (3b) are characterized in the bubble chamber by a vertex at which the slow, heavy incident

$K^-$  track ends, and two tracks, the lightly ionizing pion and a short ( $\leq 1.2$  cm) heavy  $\Sigma$  originate. The ending of a  $\Sigma$  track is characteristically associated with a lightly ionizing track, the decay pion, or with a stopping positive track, characterizing the case of  $\Sigma^+ \rightarrow \pi^0 + p$  decay in reaction (3a). If the kaon is captured at rest, as is the case in 90% of the capture events, the  $\Sigma$  and the capture pion are collinear.<sup>12</sup> It also happens not too infrequently that the  $\Sigma$  track is too short to be seen and the kaon ends in a vertex with two outgoing tracks. Such events are called here "zero-length  $\Sigma$ " (or Z.L.  $\Sigma$ ) and will also be used in the use subsequent analysis. The reason why we are able to this type of event is that apart from reactions (3a) and (3b) other mechanisms such as  $\Sigma^0 \rightarrow \Lambda^0 + e^+ + e^-$  and  $K_1^0 \rightarrow \pi^+ + \pi^-$  (with very short  $K_1^0$ ) etc., which are known to produce this type of vertex are very rare and obviously distinguishable from (3a) and (3b). If the positive track happens to be a proton, the event could be an example of



However, the distinction between (4a) and (4b) and (4c) can always be resolved either visually, as when a scattered  $K^-$  interacts, or kinematically, as is the case with short  $\Lambda^0$  decay.<sup>13</sup> Therefore, all events on the film which could be examples of reactions (3a) and (3b), whether at rest or in flight, and whether or not the  $\Sigma$  was visible, were measured. The measurements of the track coordinates in the three views were processed through by the NP54 which performed a spatial reconstruction of the individual tracks of each event.<sup>14</sup>

### C. Analysis Techniques

Since all events on the film which could be examples of reactions (3a) and (3b) were measured, it is not *always* possible to identify every event by the presence of the  $\Sigma$  track and its collinearity with respect to the corresponding capture pion. Presumably, most of the information useful for a systematic analysis of the events is carried by the two oppositely charged prongs, the capture pion and the decay track of the  $\Sigma$ . Based on the measured vector momenta of these two tracks,

<sup>12</sup> This kind of event will be referred to as "collinear  $\Sigma$ 's" in the subsequent analysis. For  $K^- + p$  interaction in flight, the  $\Sigma$  and the capture pion are not collinear; they will be referred to as "noncollinear  $\Sigma$ 's."

<sup>13</sup> Obviously identifiable short length  $\Lambda^0$  events from reaction (4b) have been rejected during the stage of scanning.

<sup>14</sup> NP54 is a geometrical reconstruction program for bubble-chamber tracks, which was written originally by Professor R. Plano and is now maintained by F. Wuensch, Nevis Laboratories.

<sup>10</sup> C. Alff, N. Gelfand, U. Nauenberg, M. Nussbaum, J. Schultz, J. Steinberger, H. Brugger, L. Kirsch, R. Plano, D. Berley, and A. Prodell, Phys. Rev. **137**, B1105 (1965).

<sup>11</sup> The  $K^-$  beam transport system was described in detail in the appendix of Ref. 10. For the features of the Columbia-BNL 30-in. hydrogen bubble chamber, see, for instance, R. P. Shutt, in *Proceedings of the 1962 International Conference on Instrumentation for High Energy Physics at CERN*, edited by F. J. M. Farley (North-Holland Publishing Company, Amsterdam, 1963).

a kinematic fit to the following hypotheses for  $K^-$  capture at rest:

$$\text{Hypothesis A: } K^- + p \rightarrow \Sigma^+ + \pi^- \quad (5a)$$

$$\searrow$$

$$\pi^+ + n;$$

$$\text{Hypothesis B: } K^- + p \rightarrow \Sigma^- + \pi^+ \quad (5b)$$

$$\searrow$$

$$\pi^- + n;$$

$$\text{Hypothesis C: } K^- + p \rightarrow \Sigma^+ + \pi^- \quad (5c)$$

$$\searrow$$

$$\pi^0 + p,$$

plus the ionization information carried by the positively charged prong should be able to distinguish one event from the other. But this is not obvious if the  $\Sigma$  is too short to be seen. In order to guarantee a physically significant identification of the Z.L.  $\Sigma$  events, events with clearly visible  $\Sigma$  and well-measured kinematic variables are used to deduce the properties of the Z.L.  $\Sigma$ 's. For this purpose:

(i) A Lorentz transformation has been introduced; this transformation moved the  $\Sigma$  decay prong of an event with visible  $\Sigma$  length from the vertex of decay up to the vertex of production, thus simulating a Z.L.  $\Sigma$ ; kinematic properties of these transformed events have been carefully analyzed.

(ii) Only those well-measured events selected by the geometrical restrictions which should not themselves bias the measurement of the  $\Sigma$  lifetime were accepted for the final calculations. The geometrical restrictions will be discussed in detail. For  $\Sigma^+ \rightarrow \pi^0 + p$  decays, the detection efficiency of the protons depends on the  $\Sigma^+$  velocity and the geometrical configurations of the events. Special selection criteria which insured an equal detection efficiency for all  $\Sigma^+ \rightarrow \pi^0 + p$  decays will be discussed and applied in this analysis.

### 1. Lorentz Transformation of the $\Sigma$ Decay Prong

For a heavy, charged  $\Sigma$  hyperon traveling a short distance ( $\leq 1.2$  cm) in a magnetic field of  $\sim 14$  kG,<sup>15</sup> the change in direction of motion is negligibly small. Therefore, based on the four-momentum  $q$  of the  $\Sigma$  decay prong, the velocity change of the  $\Sigma$  and the direction of the capture pion, a simple Lorentz transformation

$$q' = \mathcal{L}(\beta_i)q \quad (6)$$

is enough to enable one to calculate the four-momentum  $q'$  of the decay prong for a collinear  $\Sigma$  if it were decayed immediately after its production. In Eq. (6),  $\mathcal{L}(\beta_i)$  is the transformation matrix for an ordinary Lorentz transformation with a transformation velocity  $\beta_i$

given by<sup>16</sup>

$$\beta_i = -\frac{\beta_1 - \beta_0}{1 - \beta_1 \beta_0} \mathbf{e}_\pi, \quad (7)$$

where  $\beta_0$ =initial velocity of  $\Sigma$ ,  $\beta_1$ =final velocity of  $\Sigma$  at the vertex of  $\Sigma$  decay,  $\mathbf{e}_\pi$ =unit vector in the opposite direction of the capture pion. For noncollinear  $\Sigma$  events, we replace this direction by the direction of  $\Sigma$  obtained from a 3C fit for the  $\Sigma\pi$  production at the vertex of  $K^-$  capture. Thus the configuration of the transformed events simulates a Z.L.  $\Sigma$  event.

### 2. Geometrical Restrictions

After the Lorentz transformation of the  $\Sigma$  decay prong, the collinear  $\Sigma^+$  and  $\Sigma^-$  events are subjected to the following selection criteria:

#### Criteria I.

- (a)  $|\pi^\pm$  and proton dip angles  $|\langle 60^\circ$ .
- (b) |angles between  $K^-$  and the two outgoing prongs  $|\langle 20^\circ$ .
- (c) Production vertex lies inside a fiducial volume defined by a coaxial cylindrical volume inside the bubble chamber with its top and bottom ends 3 cm away from the chamber glasses and with its cylindrical surfaces 10 cm away from the chamber's wall.
- (d) If  $t$ =the proper time of  $\Sigma$ , then we require  $0.30 \times 10^{-10} \text{ sec} < t \leq t_m$ , where

$$t_m = 3.00 \times 10^{-10} \text{ sec for } \Sigma^+; \quad (8a)$$

$$t_m = 2.70 \times 10^{-10} \text{ sec for } \Sigma^-. \quad (8b)$$

- (e) Positively charged track is not a proton (Table I).
- (f)  $l_{\pi^\pm} \geq 8$  cm.
- (g)  $\theta_{\Sigma\pi}$  in the rest frame of  $\Sigma > 10^\circ$ .

Collinear  $\Sigma^+$ 's rejected by selection criteria I will be further examined by the following criteria:

TABLE I. Distinction between  $\pi^+$  and protons in  $\Sigma^+ \rightarrow \pi N$  decays.<sup>a</sup>

	$p_{\pi^+}$ (MeV/c)	$R_{\pi^+}$ (Ioz)	$p_p$	$R_p$ (Ioz)
When $\Sigma^+$ decays at rest	189.1	200 cm(0)	189.6	2.9 cm(3)
When $\Sigma^+$ decaying forward with $\beta_{\Sigma^+}=0.151$	220	290 cm(0)	337	23 cm(2,3)
When $\Sigma^+$ decaying backward with $\beta_{\Sigma^+}=0.151$	150	115 cm(0,1)	45	0 (3)

<sup>a</sup>  $p$ =momentum of the decay particle;  $R$ =range of the particle in hydrogen; Ioz=ionization number assignment of the track: 0=minimum (comparable to the background tracks— $\pi^-$  or  $\mu^-$ ), 1=twice minimum, 2=black, 3=stopping proton, 4=a definite pion characterized by its decay.

<sup>15</sup> The 30-in. Columbia-BNL hydrogen bubble chamber is located in a magnetic field which is approximately 13.6 kG in the center region of the chamber.

<sup>16</sup> When we speak of the velocity  $\beta$  of some particle, we always mean the ratio of the velocity of this particle to the velocity of light. It is therefore a pure number and always smaller than 1.

*Criteria II.* Restrictions (a) to (d) are the same.

(e) Positively charged track is identified as a proton and  $\cos\theta_{\pi^-p} < 0$ .

(f)  $l_{\pi^-} \geq 8$  cm,  $l_p \geq 0.4$  cm.

(g)  $\theta_{\Sigma^+p}$  in the rest frame of  $\Sigma^+ > 10^\circ$ .

Thus, any  $\Sigma$  with decay time  $\leq 0.30 \times 10^{-10}$  sec, as calculated from its measured length, is rejected by (d) in the above selection criteria. They are lumped into the category of Z.L.  $\Sigma$ 's. However, all Z.L.  $\Sigma$ 's are subjected to the following selection criteria:

*Criteria III.* Restrictions (a) through (c) are the same.

(d)  $t \leq 0.30 \times 10^{-10}$  sec.

(e) If positive track is identified as a proton, then  $\cos\theta_{\pi^-p} < 0$ . If it is a  $\pi^+$ , then  $\cos\theta_{\pi^+\pi^-}$  must lie outside the region specified by

$$-0.4 < \cos\theta_{\pi^+\pi^-} < 0.8. \quad (9)$$

(f)  $l_{\pi^+} \geq 15$  cm,  $l_p \geq 0.4$  cm, if the positive track is a proton.

(g)  $\theta_{\Sigma\pi}$  (or  $\Sigma p$ ) in the rest frame of  $\Sigma > 10^\circ$ .

Restrictions (a), (b), (f), and (g) are necessary for a precise measurement of the essential kinematic vari-

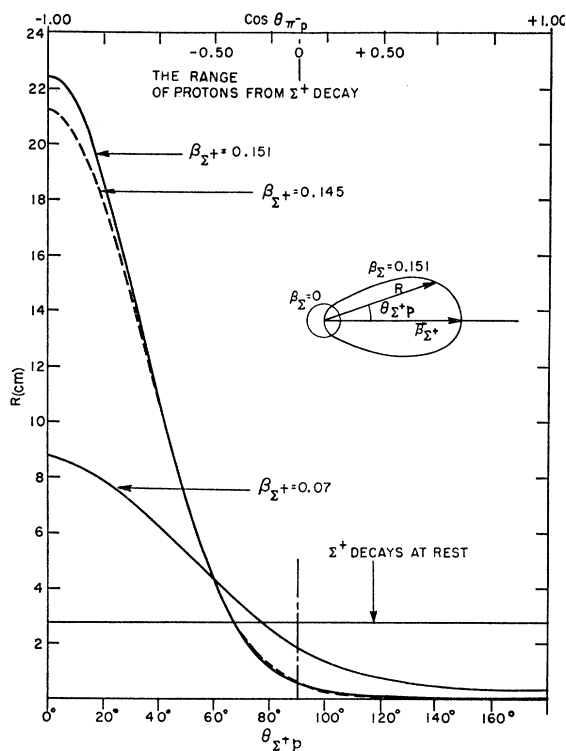


FIG. 1. The ranges of protons in hydrogen bubble chamber from  $\Sigma^+$  decays for various  $\Sigma^+$  velocities  $\beta_{\Sigma^+}$ .

ables. Condition (d) defines Z.L.  $\Sigma$ . The physical significance of the "cosine" conditions, on the other hand, will be discussed in detail as follows:

*The condition  $\cos\theta_{\pi^-p} < 0$ .* In the case of  $\Sigma^+ \rightarrow \pi^0 + p$  decays, the detection efficiency of the protons is a function of the decay angle and the velocity of  $\Sigma^+$ . This relation is clearly shown in Fig. 1, where correlations between the proton range and the decay angles are plotted for various values of  $\beta_{\Sigma^+}$ . Now, in the region  $\cos\theta_{\pi^-p} < 0$ , the minimum range of the protons from  $\Sigma^+$  decays is  $\sim 0.4$  cm; therefore the detection efficiency should be guaranteed to be equal. Outside this region, all protons should stop inside the chamber because of the fiducial volume (c); consequently, with this " $\cos\theta_{\pi^-p} < 0$ " condition, all  $\pi^+$ 's should be distinguishable from protons from  $\Sigma^+$  decays (see Table I).

*The condition  $-0.4 < \cos\theta_{\pi^+\pi^-} < 0.8$ .* Suppose all of the transformed events surviving selection criteria I and II, regardless of the appearance of the  $\Sigma$  track, are tested for their kinematic compatibility with the hypotheses A, B, and C as they are defined in (5a), (5b), and (5c),

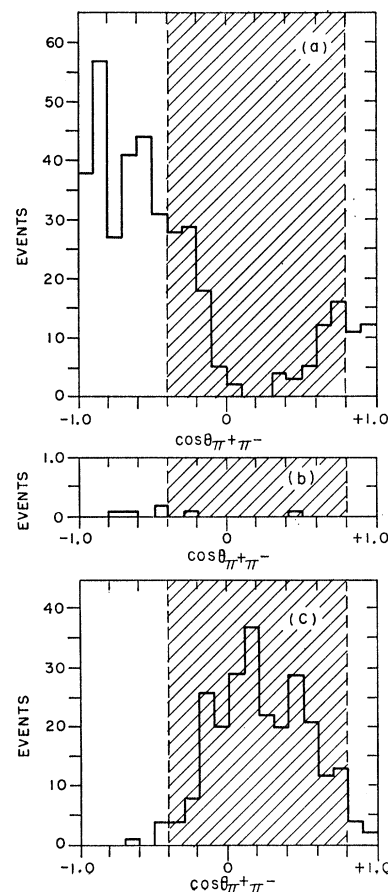


FIG. 2. Histograms of well-measured collinear  $\Sigma^+$ 's. (Collinear  $\Sigma^+ \rightarrow \pi^+ + n$  events surviving selection criteria I.) (a) Fit hypothesis A only. (b) Fit hypothesis B only. (c) Fit both hypotheses A and B.

TABLE II. Summary of the events.

Event types <sup>a</sup>	Collinear $\Sigma^+$		Collinear $\Sigma^-$	Zero-length $\Sigma^\pm$			Noncollinear $\Sigma^+$		Noncollinear $\Sigma^-$
Measured	2157		4907	2132			334		434
Accepted by NP54	2019		4774	2074			322		415
Survived I	558	...	2535	...			...		...
Survived II	...	582	...	...			...		...
Survived III	178	498	795	287	279	12	48	48	
Survived I (or II) and fit X	534	567	2490						
Survived III and fit X	173	475	777	75	191	207	6	11	20
where X=	A	C	B	A	B	C	A	C	B
Detection efficiency $\epsilon^b$	0.318	0.816	0.313	...	...	...	...		...

<sup>a</sup> I, II, and III represent the selection criteria and X=A, B, or C represent the hypothesis numbers. The acceptance of an event for an hypothesis is that  $\chi_{2s}^2(x) \leq 6.0$ .

respectively. Every event as a whole can be tested by a  $2C$  class fit to each hypothesis with an over-all  $\chi^2(x)$  given by the sum<sup>17</sup>

$$\chi^2(x) = \chi_{\text{prod}}^2(x) + \chi_{\text{decay}}^2(x), \quad (10)$$

where  $x$ =hypothesis A, B, or C. According to the  $\chi^2$ 's, each event, e.g., a transformed collinear  $\Sigma^+ \rightarrow \pi^+ + n$ , should either be accepted by A and rejected by B, or be accepted by both, or vice versa. Such results are shown by the histograms in Fig. 2, where the shadings indicate the kinematically ambiguous regions for Z.L.  $\Sigma$ 's. To convince oneself that this ambiguity is an inherent property of reactions (3a) and (3b) from  $K^-$  capture at rest, the momentum spectrum of the  $\pi^+$ 's in the Z.L.  $\Sigma^+ \rightarrow \pi^+ + n$  decays is plotted in Fig. 3(a). In the shaded region, the decay  $\pi^+$ 's have the same momentum as the capture  $\pi^+$ 's associated with  $\Sigma^-$  production from  $K^-$  capture at rest in reaction (3b). By cutting off these events inside the region specified by Eq. (9), there will be no ambiguity in the identification of the remaining 43% of Z.L.  $\Sigma$ 's for the  $\Sigma^\pm \rightarrow \pi^\pm + n$  decays.

### 3. Subtraction of the In-Flight $K^-$ Interaction Contaminations for Z.L. $\Sigma$ 's

After the Lorentz transformation of the  $\Sigma$  decay prong, all the obviously noncollinear  $\Sigma$  events were subjected to selection criteria similar to criteria III except that the condition III (a) was replaced by " $t > 0.30 \times 10^{-10}$  sec." The surviving events were further examined by the corresponding hypothesis A, B, or C, respectively. The  $\chi^2$ 's obtained from the kinematical fittings showed that the kinematics rejected most but not all of the  $K^-$  in-flight interaction events. Suppose  $N_f(x)$  of these events satisfied hypothesis  $x$ , and  $N_r(x)$  collinear  $\Sigma$ 's of the same type  $x$  which survived the same selection criteria also satisfied hypothesis  $x$ , where  $x$ =A, B, or C. Then multiplying the number of Z.L.  $\Sigma(x)$ 's selected by the selection criteria III by a

factor

$$\epsilon_f(x) = \frac{N_r(x)}{N_r(x) + N_f(x)}, \quad (11)$$

we will obtain the corrected number of Z.L.  $\Sigma(x)$ 's which is free from the contamination introduced by  $K^-$  interaction in flight.

## III. RESULTS

### A. Tabulation of the Number of Events Surviving the Various Selection Criteria

The number of events which have been found in approximately 10 000 pictures are tabulated in Table II.

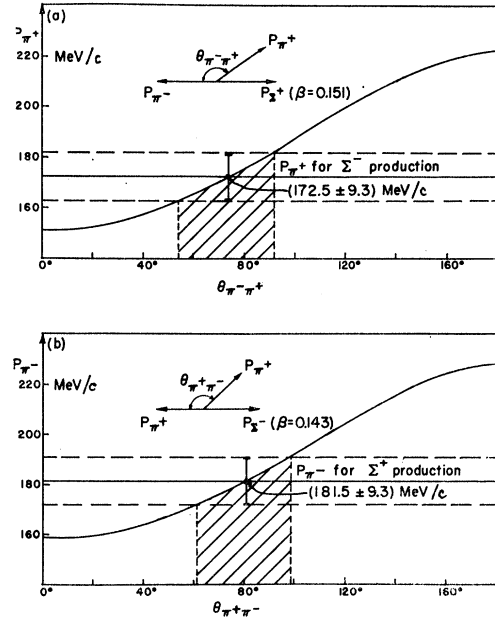


FIG. 3. (a) The  $\pi^+$  momentum spectrum calculated from  $\Sigma^+$  decay with  $\beta_{\Sigma^+} = 0.511$ . In the shaded region the  $\pi^+$  in  $\Sigma^+ \rightarrow \pi^+ + n$  has the same momentum of the capture  $\pi^+$ , which is associated with the production of  $\Sigma^-$  in  $K^- + p \rightarrow \Sigma^- + \pi^+$ . (b) The  $\pi^-$  momentum spectrum calculated from  $\Sigma^- \rightarrow \pi^- + n$  decay with  $\beta_{\Sigma^-} = 0.143$ . The momentum for the capture  $\pi^-$  is 181.5 MeV/c.

<sup>17</sup> By means of the least-squares method, GRIND computed the best solution for a kinematical fitting for each hypothesis; GRIND is an IBM 7094 program written at CERN.

### B. The Detection Efficiencies

In the case of lifetime calculations, collinear  $\Sigma$ 's have a detection efficiency independent of the  $\Sigma$  decay time due to the fact that all geometrical restrictions were applied to the events after a Lorentz transformation of the  $\Sigma$  decay prongs. The detection efficiencies  $\epsilon_0$ 's of Z.L.  $\Sigma(x)$ 's were obtained by comparing the numbers of survived collinear  $\Sigma$ 's when selection criteria III and I (or II) were applied. The computed ratios are shown in the last row of Table II. According to Eq. (11), and using the numbers shown in the second line from the bottom of Table II, we have also calculated the correction factors for Z.L.  $\Sigma$ 's due to  $K^-$  in-flight interaction contaminations. The corrections are

$$\begin{aligned}\epsilon_f(\text{A}) &= 96.7\% \text{ for } \Sigma^+ \rightarrow \pi^+ + n, \\ \epsilon_f(\text{B}) &= 97.5\% \text{ for } \Sigma^- \rightarrow \pi^- + n, \\ \epsilon_f(\text{C}) &= 97.8\% \text{ for } \Sigma^+ \rightarrow \pi^0 + p.\end{aligned}\quad (12)$$

For the computation of the branching ratio  $B_{\Sigma^+}$ , the detection efficiency for the protons relative to that of the  $\pi^+$ 's was given by<sup>18</sup>

$$\begin{aligned}\epsilon &= \frac{(\text{selection criteria II})}{(\text{selection criteria I})} \\ &= \frac{(\text{condition } \cos\theta_{\pi-p} < 0)}{(\text{condition for } \pi^+ \text{ length cutoff})} \\ &= 0.914.\end{aligned}\quad (13)$$

### C. The Calculation of the Decay Time

For  $K^-$  capture at rest, the  $\Sigma$  hyperon has a well-known initial momentum in the laboratory. From the known initial momentum, the rate of energy loss and the measured length of  $\Sigma$  in liquid hydrogen, the decay time was evaluated numerically in the rest frame of  $\Sigma$  as follows:

$$\begin{aligned}t &= \int_0^l dx / \gamma v(x) \\ &= \left( \frac{mc^2}{c} \right) \int_0^l \frac{dx}{cp(x)},\end{aligned}\quad (14)$$

where  $t$  = the  $\Sigma$  proper decay time, in seconds,  $x$  = distance from the production vertex, in centimeters,  $l$  =  $\Sigma$  length, in centimeters,  $mc^2$  = rest mass of  $\Sigma$ , in MeV,  $c$  = velocity of light in vacuum =  $3 \times 10^{10}$  cm/sec,  $p(x)$  = momentum of  $\Sigma$  at a distance  $x$  from the vertex of  $K^-$  capture in MeV/c. Table III shows the computed decay time for  $\Sigma^\pm$  as a function of the measured length of  $\Sigma$  in liquid hydrogen. Essential constants

<sup>18</sup> For  $\beta_{\Sigma^+} = 0.151$ , the condition " $\cos\theta_{\pi-p} < 0$ " in the laboratory system is equivalent to " $\theta_{\Sigma^+p} \text{ c.m.} < 140^\circ$ " in the rest frame of  $\Sigma^+$ . From the isotropic distribution of  $\Sigma^+ \rightarrow \pi^0 p$  decays in the rest frame of  $\Sigma^+$ , we find 88.3% of the total number of events survived the condition " $\cos\theta_{\pi-p} < 0$ ."

employed for this computation are also specified in this table.<sup>19</sup>

### D. The $\Sigma$ Lifetime

The  $\Sigma$  lifetime was determined by means of the least squares method. This method consists of evaluating the  $\Sigma$  mean lifetime  $\tau$  by minimizing a  $\chi^2$  function defined by

$$\chi^2(\tau) = \frac{[N_0/\epsilon_0 - \bar{N}(1, \tau)]^2}{\bar{N}(1, \tau)} + \sum_{n=2}^m \frac{[N_n - \bar{N}(n, \tau)]^2}{\bar{N}(n, \tau)}, \quad (15)$$

where  $N_0$  = number of Z.L.  $\Sigma$ 's observed under selection criterion III,  $\epsilon_0$  = detection efficiency for Z.L.  $\Sigma$ 's defined in Sec. III-B divided by the corresponding  $\epsilon_f$  given by Eq. (12),  $N_n$  = number of  $\Sigma$  decays observed in the  $n$ th time interval on the differential decay time distribution, where  $n = 2, \dots, m$ ,  $\bar{N}(n, \tau)$  = number of events expected in the  $n$ th time interval on the distribution for a given  $\Sigma$  mean life  $\tau$ , and  $\tau$  =  $\Sigma$  mean lifetime to be considered as a parameter. Using the probability function

$$P(t, \tau) dt = \frac{e^{-t/\tau}}{\tau(1 - e^{-tm/\tau})} dt, \quad (16)$$

TABLE III. The  $\Sigma^\pm$  decay time.

$\Sigma$ length (cm)	Decay time ( $10^{-12}$ sec)	
	$\Sigma^+$	$\Sigma^-$
0.01	002.2	002.3
0.05	011.0	011.6
0.10	022.1	023.4
0.15	033.4	035.3
0.20	044.7	047.5
0.25	056.3	059.8
0.30	068.0	072.4
0.35	079.8	085.1
0.40	091.9	098.2
0.45	104.1	111.5
0.50	116.5	125.2
0.55	129.2	139.2
0.60	142.1	153.6
0.65	155.3	168.4
0.70	168.8	183.8
0.75	182.6	199.8
0.80	196.8	216.6
0.85	211.5	234.4
0.90	226.6	253.6
0.94	239.1	270.4
1.00	258.8	...
1.05	276.1	...
1.10	294.6	...
	Initial momentum	Max. range
	Mass (MeV)	(MeV/c)
$\Sigma^+$	1189.4	181.538
$\Sigma^-$	1197.4	172.968
	The scale factor $S = 1.063$	
		(cm)
		1.265
		1.040

<sup>19</sup> The  $\Sigma$  masses and the scale factor  $S$  employed in this calculation are based on the values recently determined by P. Schmidt, Phys. Rev. **140**, B1328 (1956). The scale factor  $S$  is defined as the ratio of the hydrogen density of the 30-in. Columbia-BNL hydrogen bubble chamber and the density assumed for range energy table in GRIND.

and integrating Eq. (16) over the time interval

$$[(n-1)\Delta t, n\Delta t],$$

we obtain

$$\bar{N}(n, \tau) = I_{\text{tot}} \int_{(n-1)\Delta t}^{n\Delta t} P(t, \tau) dt, \quad (17)$$

where  $I_{\text{tot}}$  = total number of events observed in  $(0, t_m)$ ,  $t_m$  = the potential decay time for  $\Sigma^\pm$ , which has been defined in Eqs. (8a) and (8b). However, the statistical errors in the denominators of Eq. (15) can be approximated by

$$\left[ \left( \frac{N_0}{\epsilon_0^2} \right) + \left( \frac{N_0}{\epsilon_0^2} \right)^2 \langle \delta \epsilon_0^2 \rangle_{\text{av}} \right]^{1/2} \quad \text{for } n=1, \quad (18a)$$

and by

$$N_n, \quad \text{for } n=2, \dots, m. \quad (18b)$$

Substituting Eqs. (8) and (17) into (15), and using Eq. (12) and the corresponding differential decay distribution, we can calculate the values of  $\chi^2$  as a function of  $\tau$ . The  $\Sigma$  mean lifetimes thus obtained from the minimum  $\chi^2$  solutions are

$$\tau_{\Sigma^+ \rightarrow \pi^+ + n} = (0.830 \pm 0.025) \times 10^{-10} \text{ sec}, \quad (19a)$$

$$\tau_{\Sigma^- \rightarrow \pi^- + n} = (1.648 \pm 0.026) \times 10^{-10} \text{ sec}, \quad (19b)$$

$$\tau_{\Sigma^+ \rightarrow \pi^0 + p} = (0.831 \pm 0.026) \times 10^{-10} \text{ sec}. \quad (19c)$$

Figures 4, 5, and 6 show the corresponding differential decay-time distributions.

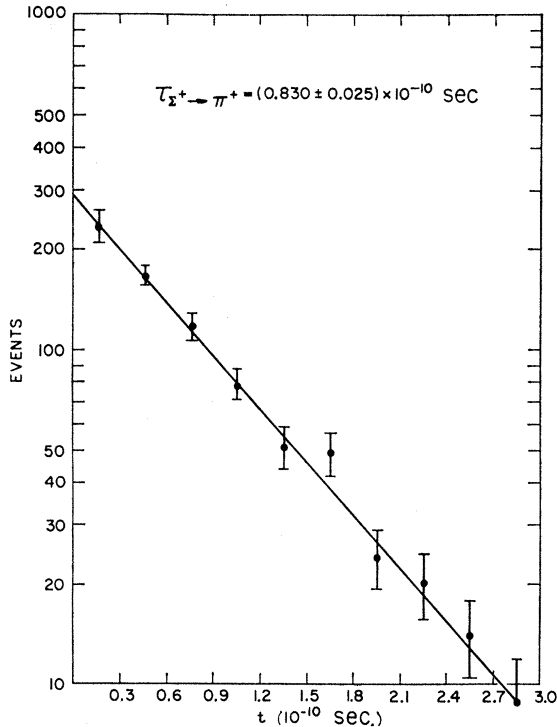


FIG. 4. Differential decay-time distribution for  $\Sigma^+ \rightarrow \pi^+ + n$ .

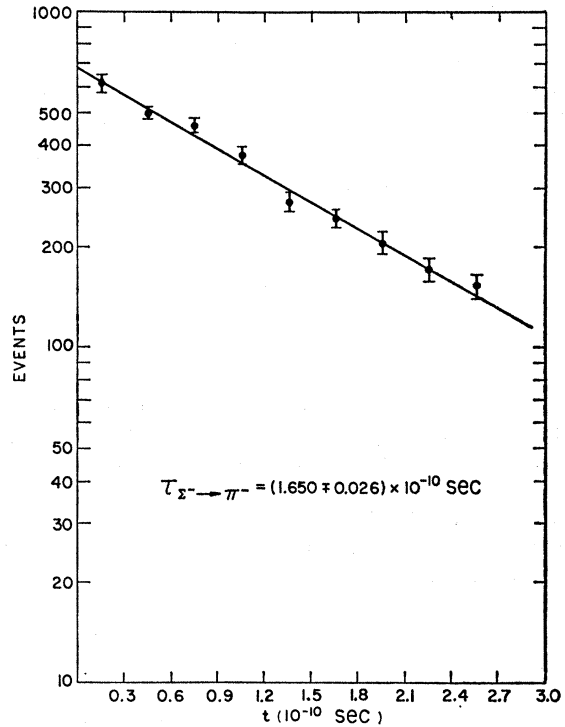


FIG. 5. Differential decay-time distribution for  $\Sigma^- \rightarrow \pi^- + n$ .

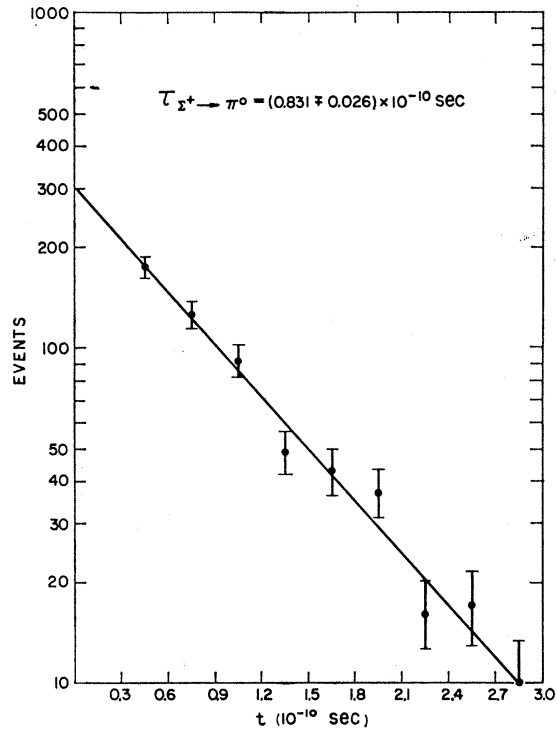


FIG. 6. Differential decay-time distribution for  $\Sigma^+ \rightarrow \pi^0 + p$ .

### E. The Effect of $\Sigma^- + p$ Interactions on the Determination of $\Sigma^-$ Lifetime

Because of  $(\Sigma^- + p)$  interactions, the  $\Sigma^-$  flux attenuates according to the statistical law

$$\begin{aligned} d\bar{N} &= -N \left( \frac{1}{\tau} + n_0 \sigma \frac{dx}{dt} \right) dt \\ &= -N \left( \frac{1}{\tau} + n_0 c \beta \sigma \right) dt \\ &\equiv -NS(\tau, \sigma, t) dt, \end{aligned} \quad (20)$$

where  $N$  = intensity of the  $\Sigma^-$  flux at time  $t$ ,  $n_0$  = number of nuclear interactions centers per cc,  $\beta$  =  $\Sigma^-$  velocity,  $\sigma$  = total cross section for  $\Sigma^- + p$  interactions. Thus, a more general probability function than Eq. (16) for observing an individual event, either decay or nuclear interaction at time  $t$  to  $t + dt$  can be derived from Eq. (20) as follows:

$$P(\tau, \sigma, t) dt = \frac{S(\tau, \sigma, t) \exp\left(-\int_0^t S(\tau, \sigma, \xi) d\xi\right)}{1 - \exp\left(-\int_0^{t_m} S(\tau, \sigma, \xi) d\xi\right)} dt. \quad (21)$$

The reactions  $\Sigma^- + p \rightarrow (\Lambda^0, \Sigma^0) + n$  which dominates the low-energy  $\Sigma^- + p$  interactions has recently been studied by several groups.<sup>20</sup> From the cross section  $\sigma(\Sigma^- + p \rightarrow$

$(\Lambda^0, \Sigma^0) + n$ ), the interaction rates for  $\Sigma^- + p$  were estimated as shown in Fig. 7. Using Eq. (21) and Fig. 7, and a numerical calculation similar to that of the previous section, we obtain

$$\tau_{\Sigma^-} = (1.666 \pm 0.026) \times 10^{-10} \text{ sec.} \quad (22)$$

### F. The Branching Ratio $B_{\Sigma^+}$

To eliminate possible contaminations introduced by short length  $\Lambda$ 's on the Z.L.  $\Sigma^+ \rightarrow \pi^0 + p$  decays, only these  $\Sigma^+$ 's with a decay time  $t > 0.30 \times 10^{-10}$  sec are used to compute the branching ratio  $B_{\Sigma^+}$ . The numbers are given in Table II; the detection efficiency  $\epsilon$  for the protons is calculated in Eq. (13). The branching ratio  $B_{\Sigma^+}$ , thus obtained from 1100 well-measured and uniquely identified collinear  $\Sigma^+$  decays, is

$$\begin{aligned} B_{\Sigma^+} &\equiv \frac{(\Sigma^+ \rightarrow \pi^+ + n)}{(\Sigma^+ \rightarrow \pi^+ + n) + (\Sigma^+ \rightarrow \pi^0 + p) / \epsilon} \\ &= \frac{534}{534 + 567/0.914} = (0.46 \pm 0.02). \end{aligned} \quad (23)$$

## IV. DISCUSSION OF THE RESULTS

To compare the present results with the previously determined  $\tau_{\Sigma^+}$  and  $B_{\Sigma^+}$ , the two independently determined  $\tau_{\Sigma^+}$ 's shown in Eq. (19a) and (19c) are combined

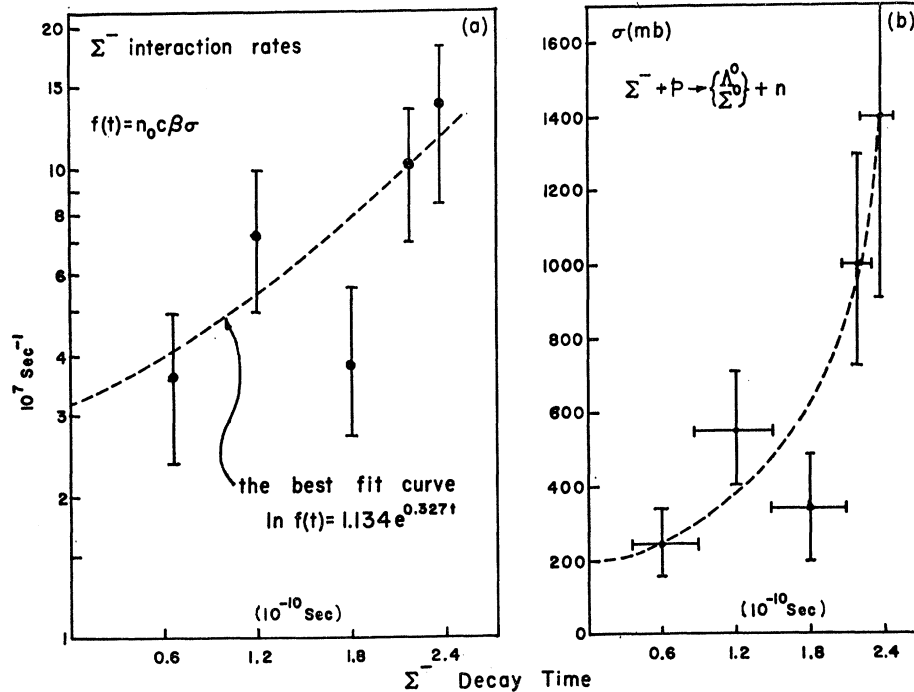


FIG. 7. (a) The interaction rates for  $\Sigma^- + p \rightarrow (\Lambda^0, \Sigma^0) + n$ . (b) The interaction cross sections for  $\Sigma^- + p \rightarrow$  neutrals. The data were obtained from Dr. J. Schultz.

<sup>20</sup> J. Schultz (private communication); R. Burnstein (private communication), see also, University of Maryland Technical Report No. 469, 1965 (unpublished).



to give

$$\tau_{\Sigma^\pm} = (0.830 \pm 0.018) \times 10^{-10} \text{ sec.} \quad (24)$$

Table IV compiled the values of Eqs. (22), (23), and (24) and the most recently published  $\tau_{\Sigma^\pm}$ 's and  $B_{\Sigma^\pm}$ 's. The lifetimes reported by Humphrey and Ross<sup>8</sup> are systematically lower than the present measurements by nearly 1.5 standard deviations. The branching ratios reported by both earlier experiments also differ from the present value by 1.5 standard deviations, which is possibly due to their ignorance of the scanning biases introduced by the short-length protons from  $\Sigma^+ \rightarrow \pi^0 + p$  decays. However, the three measurements are consistent with each other; their weighted averages are shown in the last line of Table IV.

The decay rates  $\Gamma_{\pm,0}$  for  $\Sigma^\pm \rightarrow \pi^\pm + N$  observed in this experiment computed from Eqs. (22), (23), and (24) are

$$\Gamma_+ = (0.554 \pm 0.026) \times 10^{10} \text{ sec}^{-1}, \quad (25a)$$

$$\Gamma_- = (0.600 \pm 0.009) \times 10^{10} \text{ sec}^{-1}, \quad (25b)$$

$$\Gamma_0 = (0.650 \pm 0.027) \times 10^{10} \text{ sec}^{-1}. \quad (25c)$$

The  $\Gamma$ 's and the corresponding transition matrix  $M$  defined in Eq. (2) are related by

$$\Gamma = 2\pi |M|^2 \rho, \quad (26)$$

where  $\rho$  is the integrated density of states. With the  $|\Delta I| = \frac{1}{2}$  and nonconservation of parity in weak interactions,<sup>21</sup> the transition matrix  $M$  and the decay asymmetry parameter  $\alpha$  corresponding to the decay processes [Eq. (2)] can be written explicitly in terms of four independent parameters  $S_{1/2}$ ,  $P_{1/2}$ ,  $S_{3/2}$ , and  $P_{3/2}$ ,<sup>22</sup> where  $S_I$  and  $P_I$  are the  $S$ - and  $P$ -wave amplitudes for the final states of Eq. (2) and where the  $\pi N$  system has a total isotopic spin  $I$ . Therefore, the six quantities,  $\Gamma$ 's and  $\alpha$ 's, can be overdetermined by two. The available experimental data on the  $\alpha$ 's are

$$\alpha^+ = -0.05 \pm 0.09, \quad (27a)$$

$$\alpha^- = -0.16 \pm 0.21, \quad (27b)$$

$$\alpha^0 = -0.84 \pm 0.15, \quad (27c)$$

where Eq. (27a) is the weighted average of Tripp<sup>23</sup>

<sup>21</sup> T. D. Lee and C. N. Yang, Phys. Rev. **104**, 354 (1956).

<sup>22</sup> T. D. Lee, J. Steinberger, G. Feinberg, P. K. Kabir, and C. N. Yang, Phys. Rev. **106**, 1367 (1957). See also T. D. Lee and C. N. Yang, *ibid.* **108**, 1645 (1957).

<sup>23</sup> R. D. Tripp, M. B. Watson, and M. Ferro-Luzzi, Phys. Rev. Letters **9**, 66 (1962).

TABLE IV.  $\Sigma^\pm$  lifetimes and the branching ratio  $B_{\Sigma^\pm} \equiv (\Sigma^\pm \rightarrow \pi^\pm + n) / (\Sigma^\pm \rightarrow \text{all})$ .

	$\tau_{\Sigma^+}$ ( $10^{-10}$ sec)	$\tau_{\Sigma^-}$ ( $10^{-10}$ sec)	$B_{\Sigma^\pm} = (\Sigma^\pm \rightarrow \pi^\pm + n) / (\Sigma^\pm \rightarrow \text{all})$
a	$0.830 \pm 0.018$	$1.666 \pm 0.026$	$0.46 \pm 0.02$
b	$0.765 \pm 0.04$	$1.58 \pm 0.06$	$0.49 \pm 0.02$
c	$0.82_{-0.08}^{+0.10}$	$1.75_{-0.30}^{+0.39}$	$0.50 \pm 0.03$
d	$0.819 \pm 0.016$	$1.672 \pm 0.023$	$0.47 \pm 0.01$

<sup>a</sup> The present experiment.

<sup>b</sup> W. E. Humphrey and R. R. Ross (Ref. 8).

<sup>c</sup> W. H. Barkas *et al.* (Ref. 9).

<sup>d</sup> Weighted averages.

and Cork,<sup>24</sup> Eq. (27b) is Tripp's result,<sup>23</sup> and Eq. (27c) is the weighted average of Tripp<sup>23</sup> and Keefe.<sup>25</sup> Combining Eq. (25) and Eq. (27), we have re-examined the validity of  $|\Delta I| = \frac{1}{2}$  in the nonleptonic decays of  $\Sigma$ 's by solving the four unknowns  $S_I$  and  $P_I$  from six equations in the  $\chi^2$  sense.<sup>26</sup> The best fit gives  $\chi^2 = 0.89$ . For a problem of two degrees of freedom, the probability of  $\chi^2 \geq 0.89$  is 64%, which implies excellent agreement with the  $|\Delta I| = \frac{1}{2}$  rule.

#### ACKNOWLEDGMENTS

I take great pleasure in thanking Professor J. Steinberger for his guidance and patience during the course of this experiment. I would also like to thank and express appreciation to Dr. M. Nussbaum, Dr. T. H. Tan, Dr. N. Gelfand, Dr. U. Nauenberg, and Dr. P. Schmidt for constant assistance in analysis and for illuminating discussions. The author would also like to thank the crew of the 30-in. Columbia-BNL hydrogen bubble chamber group, members of the AGS staff, and the Nevis scanners and measurers.

<sup>24</sup> B. Cork, L. Keith, W. A. Wenzel, J. W. Cronin, and R. L. Cool, Phys. Rev. **120**, 1000 (1960).

<sup>25</sup> D. Keefe *et al.*, quoted by N. P. Samios, in *Proceedings of the International Conference on Weak Interactions, 1965* (to be published). See also Brookhaven National Laboratory Report No. BNL-9666 (unpublished).

<sup>26</sup> This method was first used by Franzini and Zanello, cf. Ref. 7. Using this method and the world average experimental data available for  $\Sigma^\pm$  decays, N. P. Samios, in *Proceedings of the International Conference on Weak Interactions, Argonne National Laboratory, 1965* (to be published) has redone the problem. A similar result has been obtained. The amplitudes  $A_I$  and  $B_I$  used in the above paper are related to  $S_I$  and  $P_I$  by the equations of Samios' Table II. The experimental data used in his analysis are compiled in his Table V.